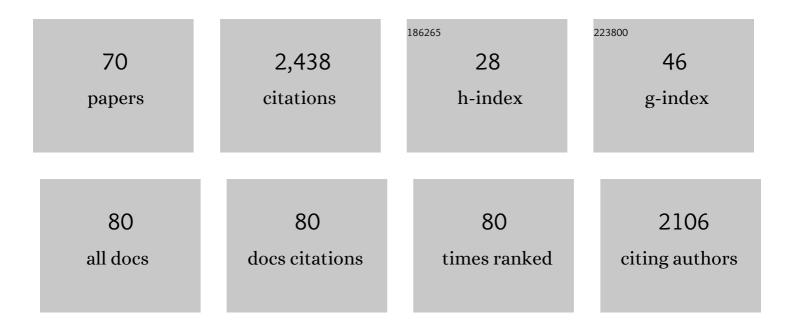
## Salim A Si-Mohamed

List of Publications by Year in descending order

Source: https://exaly.com/author-pdf/7331102/publications.pdf Version: 2024-02-01



#	Article	IF	CITATIONS
1	Comparison of image quality between spectral photon-counting CT and dual-layer CT for the evaluation of lung nodules: a phantom study. European Radiology, 2022, 32, 524-532.	4.5	26
2	Coronary calcium scoring potential of large field-of-view spectral photon-counting CT: a phantom study. European Radiology, 2022, 32, 152-162.	4.5	36
3	Comparison of two deep learning image reconstruction algorithms in chest CT images: A task-based image quality assessment on phantom data. Diagnostic and Interventional Imaging, 2022, 103, 21-30.	3.2	36
4	First In-Human Results of Computed Tomography Angiography for Coronary Stent Assessment With a Spectral Photon Counting Computed Tomography. Investigative Radiology, 2022, 57, 212-221.	6.2	62
5	Comparison of virtual monoenergetic imaging between a rapid kilovoltage switching dual-energy computed tomography with deep-learning and four dual-energy CTs with iterative reconstruction. Quantitative Imaging in Medicine and Surgery, 2022, 12, 1149-1162.	2.0	16
6	Improved coronary calcium detection and quantification with low-dose full field-of-view photon-counting CT: a phantom study. European Radiology, 2022, 32, 3447-3457.	4.5	17
7	Automatic quantitative computed tomography measurement of longitudinal lung volume loss in interstitial lung diseases. European Radiology, 2022, 32, 4292-4303.	4.5	11
8	Coronary CT Angiography with Photon-counting CT: First-In-Human Results. Radiology, 2022, 303, 303-313.	7.3	122
9	Virtual monoenergetic images from photon-counting spectral computed tomography to assess knee osteoarthritis. European Radiology Experimental, 2022, 6, 10.	3.4	15
10	Embolization of Recurrent Pulmonary Arteriovenous Malformations by Ethylene Vinyl Alcohol Copolymer (Onyx®) in Hereditary Hemorrhagic Telangiectasia: Safety and Efficacy. Journal of Personalized Medicine, 2022, 12, 1091.	2.5	3
11	Chest CT for rapid triage of patients in multiple emergency departments during COVID-19 epidemic: experience report from a large French university hospital. European Radiology, 2021, 31, 795-803.	4.5	30
12	Progressive fibrosing interstitial lung disease: a clinical cohort (the PROGRESS study). European Respiratory Journal, 2021, 57, 2002718.	6.7	103
13	Performance of four dual-energy CT platforms for abdominal imaging: a task-based image quality assessment based on phantom data. European Radiology, 2021, 31, 5324-5334.	4.5	24
14	Comparison of free breathing 3D mDIXON with single breath-hold 3D inversion recovery sequences for the assessment of Late Gadolinium Enhancement. European Journal of Radiology, 2021, 134, 109427.	2.6	2
15	Reduced-iodine-dose dual-energy coronary CT angiography: qualitative and quantitative comparison between virtual monochromatic and polychromatic CT images. European Radiology, 2021, 31, 7132-7142.	4.5	23
16	Integrated imaging evaluation in infective endocarditis: A pictorial essay on clinical cases of extracardiac complications. International Journal of Infectious Diseases, 2021, 105, 62-67.	3.3	4
17	Feasibility of human vascular imaging of the neck with a large field-of-view spectral photon-counting CT system. Diagnostic and Interventional Imaging, 2021, 102, 329-332.	3.2	31
18	Early Prediction of Cardiac Complications in Acute Myocarditis by Means of Extracellular Volume Quantification With the Use of Dual-Energy Computed Tomography. JACC: Cardiovascular Imaging, 2021, 14, 2041-2042.	5.3	11

SALIM A SI-MOHAMED

#	Article	IF	CITATIONS
19	Estimates of epidemiology, mortality and disease burden associated with progressive fibrosing interstitial lung disease in France (the PROGRESS study). Respiratory Research, 2021, 22, 162.	3.6	31
20	Feasibility of lung imaging with a large field-of-view spectral photon-counting CT system. Diagnostic and Interventional Imaging, 2021, 102, 305-312.	3.2	52
21	Diagnostic Performance of Extracellular Volume Quantified by Dual-Layer Dual-Energy CT for Detection of Acute Myocarditis. Journal of Clinical Medicine, 2021, 10, 3286.	2.4	9
22	In Vivo Molecular K-Edge Imaging of Atherosclerotic Plaque Using Photon-counting CT. Radiology, 2021, 300, 98-107.	7.3	55
23	Mise au point didactiqueÂ: l'examen clinique objectif et structuré ou «ÂECOS» en imagerie médicale. Journal D'imagerie Diagnostique Et Interventionnelle, 2021, 5, 43-43.	0.0	1
24	Lung ultrasound score as a tool to monitor disease progression and detect ventilator-associated pneumonia during COVID-19-associated ARDS. Heart and Lung: Journal of Acute and Critical Care, 2021, 50, 700-705.	1.6	17
25	Nintedanib in idiopathic and secondary pleuroparenchymal fibroelastosis. Orphanet Journal of Rare Diseases, 2021, 16, 419.	2.7	20
26	Spectral Photon-Counting CT Technology in Chest Imaging. Journal of Clinical Medicine, 2021, 10, 5757.	2.4	39
27	Performance of Spectral Photon-Counting Coronary CT Angiography and Comparison with Energy-Integrating-Detector CT: Objective Assessment with Model Observer. Diagnostics, 2021, 11, 2376.	2.6	25
28	"Dark-blood―dual-energy computed tomography angiography for thoracic aortic wall imaging. European Radiology, 2020, 30, 425-431.	4.5	11
29	mTOR inhibitors for the management of difficult lymphangioma in adults. Respiratory Medicine and Research, 2020, 77, 8-10.	0.6	1
30	Spectral Photon-Counting Computed Tomography for Coronary Stent Imaging. Investigative Radiology, 2020, 55, 61-67.	6.2	56
31	Dextran-Coated Cerium Oxide Nanoparticles: A Computed Tomography Contrast Agent for Imaging the Gastrointestinal Tract and Inflammatory Bowel Disease. ACS Nano, 2020, 14, 10187-10197.	14.6	89
32	Spectral photon-counting CT imaging of colorectal peritoneal metastases: initial experience in rats. Scientific Reports, 2020, 10, 13394.	3.3	14
33	<i>In vivo</i> demonstration of pulmonary microvascular involvement in COVID-19 using dual-energy computed tomography. European Respiratory Journal, 2020, 56, 2002608.	6.7	33
34	lodinated polymer nanoparticles as contrast agent for spectral photon counting computed tomography. Biomaterials Science, 2020, 8, 5715-5728.	5.4	15
35	Multicolor spectral photon counting CT monitors and quantifies therapeutic cells and their encapsulating scaffold in a model of brain damage. Nanotheranostics, 2020, 4, 129-141.	5.2	19
36	Head-to-head comparison of lung perfusion with dual-energy CT and SPECT-CT. Diagnostic and Interventional Imaging, 2020, 101, 299-310.	3.2	37

SALIM A SI-MOHAMED

#	Article	IF	CITATIONS
37	CT dose optimization for the detection of pulmonary arteriovenous malformation (PAVM): A phantom study. Diagnostic and Interventional Imaging, 2020, 101, 289-297.	3.2	19
38	Prolidase deficiency: a new genetic cause of combined pulmonary fibrosis and emphysema syndrome in the adult. European Respiratory Journal, 2020, 55, 1901952.	6.7	11
39	Atrial premature activity detected after an ischaemic stroke unveils atrial myopathy. Archives of Cardiovascular Diseases, 2020, 113, 227-236.	1.6	8
40	Hybrid Nano-GdF3 contrast media allows pre-clinical in vivo element-specific K-edge imaging and quantification. Scientific Reports, 2019, 9, 12090.	3.3	23
41	Virtual versus true non-contrast dual-energy CT imaging for the diagnosis of aortic intramural hematoma. European Radiology, 2019, 29, 6762-6771.	4.5	32
42	Effect of Gold Nanoparticle Size on Their Properties as Contrast Agents for Computed Tomography. Scientific Reports, 2019, 9, 14912.	3.3	157
43	What stroke image do we want? European survey on acute stroke imaging and revascularisation treatment. Health Policy and Technology, 2019, 8, 261-267.	2.5	5
44	Technical Note: Relative proton stopping power estimation from virtual monoenergetic images reconstructed from dualâ€layer computed tomography. Medical Physics, 2019, 46, 1821-1828.	3.0	16
45	Spectral Photon-Counting Computed Tomography (SPCCT): in-vivo single-acquisition multi-phase liver imaging with a dual contrast agent protocol. Scientific Reports, 2019, 9, 8458.	3.3	56
46	Five simultaneous artificial intelligence data challenges on ultrasound, CT, and MRI. Diagnostic and Interventional Imaging, 2019, 100, 199-209.	3.2	34
47	Automatic knee meniscus tear detection and orientation classification with Mask-RCNN. Diagnostic and Interventional Imaging, 2019, 100, 235-242.	3.2	89
48	Kidney cortex segmentation in 2D CT with U-Nets ensemble aggregation. Diagnostic and Interventional Imaging, 2019, 100, 211-217.	3.2	30
49	Liquid Embolic Agents in Spectral X-Ray Photon-Counting Computed Tomography using Tantalum K-Edge Imaging. Scientific Reports, 2019, 9, 5268.	3.3	23
50	Differentiation between blood and iodine in a bovine brain—Initial experience with Spectral Photon-Counting Computed Tomography (SPCCT). PLoS ONE, 2019, 14, e0212679.	2.5	26
51	Feasibility of improving vascular imaging in the presence of metallic stents using spectral photon counting CT and K-edge imaging. Scientific Reports, 2019, 9, 19850.	3.3	46
52	Neprilysin levels at the acute phase of STâ€elevation myocardial infarction. Clinical Cardiology, 2019, 42, 32-38.	1.8	12
53	Benign and malignant enlarged chest nodes staging by diffusion-weighted MRI: an alternative to mediastinoscopy?. British Journal of Radiology, 2018, 91, 20160919.	2.2	5
54	MRI-based detection of renal artery abnormalities related to renal denervation by catheter-based radiofrequency ablation in drug resistant hypertensive patients. European Radiology, 2018, 28, 3355-3361.	4.5	3

#	Article	IF	CITATIONS
55	Experimental feasibility of spectral photon-counting computed tomography with two contrast agents for the detection of endoleaks following endovascular aortic repair. European Radiology, 2018, 28, 3318-3325.	4.5	79
56	Reduction of patient radiation dose with a new organ based dose modulation technique for thoraco-abdominopelvic computed tomography (CT) (Liver dose right index). Diagnostic and Interventional Imaging, 2018, 99, 483-492.	3.2	7
57	Tibiofemoral joint congruence is lower in females with ACL injuries than males with ACL injuries. Knee Surgery, Sports Traumatology, Arthroscopy, 2018, 26, 1375-1383.	4.2	10
58	Pulmonary arteriovenous malformations in hereditary haemorrhagic telangiectasia: Correlations between computed tomography findings and cerebral complications. European Radiology, 2018, 28, 1338-1344.	4.5	23
59	Evaluation of a preclinical photon-counting CT prototype for pulmonary imaging. Scientific Reports, 2018, 8, 17386.	3.3	53
60	Multicolour imaging with spectral photon-counting CT: a phantom study. European Radiology Experimental, 2018, 2, 34.	3.4	60
61	Comparison of five one-step reconstruction algorithms for spectral CT. Physics in Medicine and Biology, 2018, 63, 235001.	3.0	53
62	Improved Peritoneal Cavity and Abdominal Organ Imaging Using a Biphasic Contrast Agent Protocol and Spectral Photon Counting Computed Tomography K-Edge Imaging. Investigative Radiology, 2018, 53, 629-639.	6.2	49
63	Assessment of candidate elements for development of spectral photon-counting CT specific contrast agents. Scientific Reports, 2018, 8, 12119.	3.3	58
64	Review of an initial experience with an experimental spectral photon-counting computed tomography system. Nuclear Instruments and Methods in Physics Research, Section A: Accelerators, Spectrometers, Detectors and Associated Equipment, 2017, 873, 27-35.	1.6	93
65	Phase-contrast MRI evaluation of haemodynamic changes induces by a coeliac axis stenosis in the gastroduodenal artery. British Journal of Radiology, 2017, 90, 20160802.	2.2	9
66	Evaluation of spectral photon counting computed tomography K-edge imaging for determination of gold nanoparticle biodistribution <i>in vivo</i> . Nanoscale, 2017, 9, 18246-18257.	5.6	89
67	Multicolor spectral photon-counting computed tomography: in vivo dual contrast imaging with a high count rate scanner. Scientific Reports, 2017, 7, 4784.	3.3	115
68	Diagnostic performance of a low dose triple rule-out CT angiography using SAFIRE in emergency department. Diagnostic and Interventional Imaging, 2017, 98, 881-891.	3.2	14
69	Vein Diameter on Unenhanced Multidetector CT Predicts Reperfusion of Pulmonary Arteriovenous Malformation after Embolotherapy. European Radiology, 2016, 26, 2723-2729.	4.5	12
70	Mesenteric cavernous hemangioma: Imaging-pathologic correlation. Diagnostic and Interventional Imaging, 2015, 96, 495-498.	3.2	5